Journal of Peptide Science
J. Peptide Sci. **7**: 579–587 (2001)
DOI: 10.1002/psc.353

Conformation of N-Terminal HIV-1 Tat (fragment 1–9) Peptide by NMR and MD Simulations

MEENA KANYALKAR[a], SUDHA SRIVASTAVA[b]* and EVANS COUTINHO[a]

[a] Department of Pharmaceutical Chemistry, Bombay College of Pharmacy, Kalina, Mumbai 400 098, India
[b] Tata Institute of Fundamental Research, Homi Bhabha Road, Colaba, Mumbai 400 005, India

Received 15 May 2001
Accepted 9 July 2001

Abstract: The *N*-terminal portion of HIV-1 Tat covering residues 1–9 is a competitive inhibitor of dipeptidyl peptidase IV (DP IV). We have used ^{1}H NMR techniques, coupled with molecular dynamics methods, to determine the conformation of this peptide in the three diverse media: DMSO-d_6, water (pH 2.7) and 40% HFA solution. The results indicate that in both DMSO-d_6 and HFA the peptide has a tendency to acquire a type I β-turn around the segment Asp^5-Pro^6-Asn^7-Ile^8. The *N*-terminal end is seen to be as a random coil. In water, the structure is best described as a left-handed polyproline type II (PPII) helix for the mid segment region Asp^2 to Pro^6. The structures obtained in this study have been compared with an earlier report on Tat (1–9).

Keywords: HIV-1 Tat; DP IV; conformation; NMR; molecular modelling; β-turn

INTRODUCTION

The human immunodeficiency virus type1 (HIV-1) has a regulatory gene called *Tat* whose translated protein is a potent transactivator of the transcription of genes, expressed from the HIV-1 long terminal repeat (LTR) [1,2]. The Tat protein is essential for viral replication. It has also been identified in the extracellular medium [3] (sera of AIDS patients). This extracellular Tat has been shown to suppress antigen as well as anti-CD3 induced activation and proliferation of human T cells [4,5].

Dipeptidyl peptidase IV (DP IV) is a transmembrane serine protease found on both T and B lymphocytes, besides natural killer cells. DP IV along with the T cell activation marker CD26 (DP IV/CD26) is involved in the degradation of bioactive peptides. The complex cleaves a peptide at its *N*-terminus by removing two amino acids, especially if the penultimate amino acid is either a proline or alanine [6]. What is interesting is the fact that Tat binds to DP IV and inhibits the cleavage of synthetic and physiological substrates [7]. It has been shown that the *N*-terminal (1–9) sequence of Tat (M^1-D-P-V-D^5-P-N-I-E^9) is responsible for the inhibition of the enzymic activity of DP IV [8,9]. Structure activity data have revealed that replacement of amino acids in positions 5 and 6 of Tat (1–9) leads to analogue with reduced inhibitory activity.

An understanding of the conformation of the Tat (1–9) sequence may shed some light on its binding to DP IV, which could be exploited to design derivatives with a higher binding affinity. We have thus undertaken a study of the conformation of Tat (1–9) in DMSO-d_6 and water (pH 2.7). Besides the two mentioned solvents, hexafluoroacetone (HFA) and trifluoroethanol (TFE) are proving invaluable media for studying biomolecular structure, function, dynamics and protein folding [10,11]. There is now strong evidence that structures seen in such solvents are similar to those adopted by the peptides in their active conformation. These solvents are also known to mimic features of the cell membrane and are suitable models for the same [10,11].

*Correspondence to: Dr S. Srivastava, National Facility for High Field NMR, Tata Institute of Fundamental Research, Homi Bhabha Road, Navy Nagar, Mumbai 400 005, India; e-mail: sudha@mailhost.tifr.res.in.

We have also studied the conformation of the peptide in HFA solution (55% H_2O: 5% D_2O: 40% HFA).

METHODOLOGY

Materials and Sample Preparation

The peptide was purchased from Bachem (Switzerland), while the solvents DMSO-d_6 and hexafluoroacetone (HFA) were purchased from Sigma Chemical Co. (USA). NMR studies were done in DMSO-d_6, water (95% H_2O: 5% D_2O, pH = 2.7) and HFA solution (55% H_2O: 5% D_2O: 40% HFA). In all three media, the peptide concentration was 3.75 mM. At this concentration, no aggregation was observed.

NMR

NMR experiments were done on a Varian Unity Plus 600 MHz FT-NMR at 298 K. For resonance assignments, two dimensional (2D) Double Quantum Filtered COrrelated SpectroscopY (DQF-COSY) [12] and TOtal Correlated SpectroscopY (TOCSY) [13] were recorded. For deducing the conformation, 2D-Nuclear Overhauser Enhancement SpectroscopY (NOESY) [14] was recorded. In the case of the water sample, solvent suppression was achieved using the WATERGATE (water suppression by Gradient Tailored Excitation) technique for TOCSY [15] and NOESY [16] experiments. The number of transients was 32 for TOCSY and NOESY, and 64 for DQF-COSY. The mixing pulse in TOCSY was achieved by the MLEV-17 scheme. For all 2D-NMR experiments the fids were digitized with 2 K points and the number of experiments in the t_1 dimension was 512. Quadrature detection in the t_1 period was achieved by the hypercomplex (STATES) method [17]. All 2D-NMR experiments were recorded with the conventional pulse sequences and a 1.5 s relaxation delay. The 2D data were processed using Felix software (v 97.0, MSI, USA) running on a Silicon Graphics O2 workstation. The fids were apodized by multiplication with a sine squared bell window function, the t_1 dimension was zero filled to give a final $2K \times 1K$ matrix prior to Fourier transformation.

$^3J_{NH\alpha}$ coupling constants were extracted from the 1D spectrum. Temperature coefficients of NH chemical shifts were calculated from two TOCSY spectra recorded at 298 K and 308 K. ^{13}C chemical shifts were obtained from the Gradient enhanced Heteronuclear Single Quantum Coherence (HSQC) [18] experiment. The NOE build-up curves were obtained from NOESY spectra recorded with mixing times of 100, 150, 200, 300 and 400 ms. Chemical shifts have been referenced to 2,2–dimethyl-2-silapentane-5-sulphonic acid (DSS) as internal standard.

Molecular Dynamics (MD) Simulations

MD simulations were done on a Silicon Graphs O2 machine with molecular modelling software *Insight II* and *Discover* from MSI, USA. Three simulations (S1, S2, S3) were carried out, each using NMR data in DMSO-d_6, water and HFA, respectively. The NOEs and coupling constants were used as restraints (*vide infra*) in a simulated annealing protocol (described below) to generate the solution structures.

An extended structure of the peptide was built with the *Biopolymer* module as the starting conformation for the simulations. The energy of the system was calculated with the CFF91 forcefield [19]. To prevent the *omega* torsions from flipping to the *cis* conformation during the simulations, a force constant of 100 kcal/mole/rad^2 was applied. The bond stretching in the energy equation was represented by a simple harmonic function. A dielectric constant of 1.0 was used for calculation of electrostatic interactions. The molecule was minimized initially to reduce any internal strain, which was followed by a 2.5 ps dynamics initialization run at 300 K. The dynamics was continued for a further period of 25 ps, during which time, frames at an interval of 1 ps were sampled and were finally subjected to energy minimization with restraints. This began with 1000 steps of steepest descents, was followed by 3000 steps of conjugate gradients and terminated with 300 steps of BFGS. At the end of this cycle, most structures had a gradient of 0.01 kcal/mole/Å or lower. In the MD simulations, the Newton's equations of motion were integrated with the Verlet algorithm [20] with a step length of 1 fs. Temperature control was achieved either by scaling the velocities or coupling to a temperature bath [21].

Distance Restraints

The NOEs were categorized as strong, intermediate and weak with corresponding distance ranges (1.8–2.7 Å), (1.8–3.5 Å) and (1.8–5.0 Å) set for the respective protons. These distances were modified for methyl and methylene groups and for aromatic rings that rotate fast on the NMR time scale. For

such a group of protons it is necessary to define a pseudoatom, which is used as a reference point for the distance restraint. Corrections for the distances to such pseudoatoms were made according to the rules initially formulated by Wüthrich *et al* [22]. Force constants for distance restraints ranged from 10 to 25 kcal/mole/Å^2. The total number of distance restraints used in the MD simulations is given in Table 1.

Dihedral Restraints

The $^3J_{NH\alpha}$ coupling constant [23] is related to the dihedral angle ϕ as expressed by the relationship: $^3J_{NH\alpha} = 6.7\cos^2\phi - 1.3\cos\phi + 1.5$.

The coupling constants were transformed to ϕ values, which were introduced as dihedral restraints allowing a range of $\pm 10^\circ$ on the calculated values, with a force constant of 50 kcal/mole/rad^2. The total number of such dihedral restraints used in the MD simulations is listed in Table 1.

Structure Refinement-IRMA and MARDIGRAS

Structure refinement was done using IRMA [24] for DMSO-d_6 and HFA while MARDIGRAS [25] was used for water sample. These are computational tools based on NMR relaxation theory. For a given molecular structure, the NOE intensities can be calculated taking into account the entire spin relaxation network and molecular flexibility. The calculated NOEs are then matched with the experimental and the structure refined iteratively so that the two closely match. The *R* factor obtained is thus a measure of the fit between the experimental and theoretical NOE intensities. MARDIGRAS is similar to IRMA, but with the additional capability of using the ROESY spectrum in structure refinement. The IRMA *R* factor is defined as

$$R = \sum_{i,j,m} \omega_{ij}(\tau_m)\left|A_{ij}^{cal}(\tau_m) - A_{ij}^{exp}(\tau_m)\right| \Big/ \sum_{i,j,m} \omega_{ij}(\tau_m) \times \left|A_{ij}^{exp}(\tau_m)\right|$$

where $A_{ij}^{cal}(\tau_m)$ and $A_{ij}^{exp}(\tau_m)$ denote respectively the theoretical and experimental NOE intensities for the pair (i,j) for the mixing time τ_m. The weight factors ω_{ij} account for measurement errors, particularly noise levels, and are set to 1.0. The *R* factor in MARDIGRAS is given by a similar equation.

The rotational correlation time τ_c for the molecule was estimated as 2.0 ns for DMSO from the NOE build up for the amide NH of Asn^7 and for water and

Table 1 Summary of Experimental Restraints and Statistical Analysis of the Family of Structures Generated by Simulated Annealing

Parameter	Value in different solvents		
Distance restraints	(S1) DMSO-d_6	(S2) Water	(S3) HFA
All	57	54	62
Intra-residue	39	32	27
Inter-residue	18	22	35
Sequential	6	6	7
Medium range	12	16	28
Dihedral restraints	7	7	7
Avg. fractional violation/constraint	0.0035	0.0045	0.023
Avg. no. of violations[a]/structure	1.92	1.68	4.5
RMSDs with avg. Structure: Backbone atoms			
Maximum	1.875	0.843	1.88
Minimum	0.498	0.148	1.29
Average	0.804	0.248	1.68
Average pair-wise RMSD	1.12(±0.6)	0.29(±0.4)	1.88(±1.3)
IRMA/MARDIGRAS *R*-factor	0.548	0.787	0.74

[a] $A \pm 0.2$ Å difference from the imposed distance restraint was considered a violation.

HFA, τ_c was calculated as 1 ns from the NOE build up for the CγH of Ile[8].

RESULTS AND DISCUSSION

In all three media — DMSO-d_6, water (pH 2.7) and HFA — the 1D and 2D spectra showed two or more sets of peaks arising from Asp[2], Val[4], Asp[5], Asn[7] and Ile[8] indicating the presence of other conformers in equilibrium with the major. The minor conformations have been estimated at 5–9% of the major, by integration of the cross peaks in the TOCSY spectra.

The spin systems of the various amino acids residues in the peptide are unique and were easily identified in the TOCSY spectra for each of the three different media. As an example the TOCSY spectrum in DMSO-d_6 is given in Fig. 1. Thus Met[1], Pro[3], Val[4], Ile[8] and Glu[9] could be distinguished. Asp[2,5] and Asn[7] which both have the AMX spin-system were identified as a group. Sequence specific assignments were made using the NOESY spectrum where the 'COSY' cross peak (NH-CαH) of residue i was linked to the NOE peak (CαH$_i$- NH$_{i+1}$) of the neighbouring residue ($i+1$) (Fig. 2 shows NOESY spectrum in DMSO-d_6). The presence of Pro residues at positions 3 and 6 in the peptide chain causes a break in the assignment. This was bridged by identifying an NOE between Asp[2] CαH and Pro[3] CδH and similarly between Asp[5] and Pro[6]. Incidentally, these NOEs help to confirm that both the Xxx-Pro

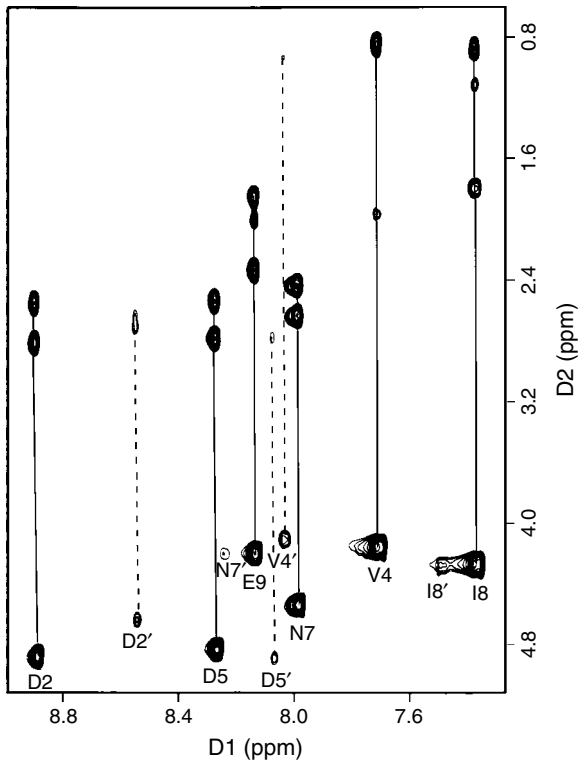

Figure 1 600 MHz TOCSY spectrum of HIV-1 Tat in DMSO-d_6 at 298 K. (D1 7.0 ppm–9.0 ppm and D2 0.6 ppm–5.0 ppm).

Table 2 Chemical Shifts (ppm) and Temperature Coefficients (ppb) of HIV-1 Tat (1–9) in DMSO-d_6

Amino acid	NH	CαH	CβH	CγH	Others	Temperature Coefficient
M[1]	—	3.88	1.98	2.51	—	—
D[2]	8.91	4.84	2.78, 2.52	—	—	3.4
D[2′]	8.54	4.62	2.72, 2.62	—	—	4.0
P[3]	—	4.44	2.01	1.90	δH 3.68	—
V[4]	7.73	4.13	—	0.88	—	4.0
V[4′]	8.03	4.08	—	0.90		4.6
D[5]	8.29	4.81	2.76, 2.51	—	—	3.8
D[5′]	8.06	4.88	2.77, 2.47	—	—	3.5
D[5″]	7.88	4.66	2.69	—	—	—
P[6]	—	4.33	2.01	1.88	δ_1H 3.72, δ_2H 3.63	—
N[7]	8.01	4.51	2.60, 2.41	—	NH$_1$ 6.96, NH$_2$ 7.33	4.0
N[7′]	8.24	4.19	2.31	—	—	—
I[8]	7.40	4.24	1.78	1.40, 1.12	δH 0.84	1.9
I[8′]	7.49	4.28	—	—	—	
E[9]	8.16	4.17	1.96, 1.83	2.31	—	4.2

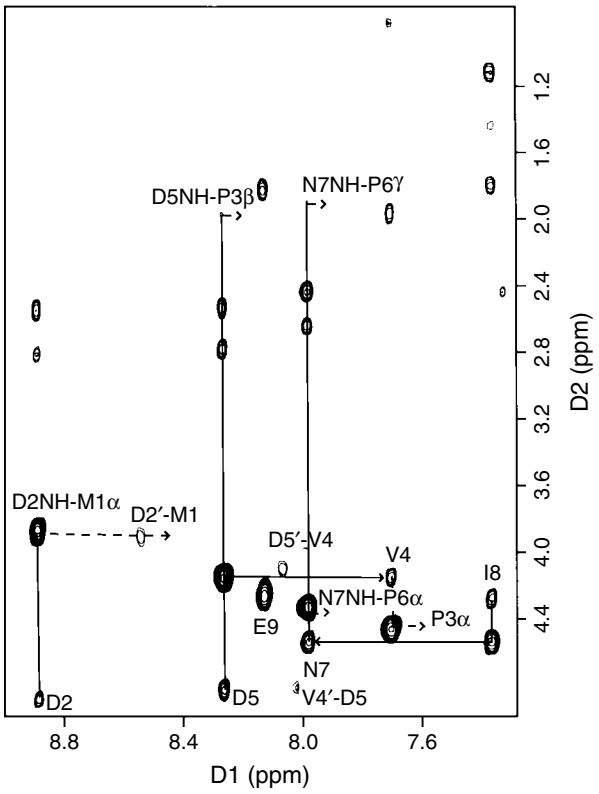

Figure 2 600 MHz NOESY spectrum of HIV-1 Tat in DMSO-d_6 recorded with mixing time of 300 ms. (D1 7.0 ppm–9.0 ppm and D2 0.8 ppm–5.0 ppm).

bonds are *trans*, [22] as are the other peptide bonds in the molecule. Thus, the major conformation of Tat (1–9) is characterized by an all *trans* peptide bond in DMSO-d_6, water and HFA.

Peptides that include prolines, often exhibit minor conformers due to *cis–trans* isomerization arising from Xxx — Pro bonds [26]. The barrier to *cis–trans* isomers is small at 16–21 kcal/mole [26] so that this transition occurs readily at room temperature. A *cis* peptide bond is identified by an NOE from the Cα proton of the residue preceding proline to the Cα proton of Pro [αH (Xxx) $\rightarrow$ αH (Pro)]. We have observed only one NOE from αH Asp^2 to αH Pro^3 for the minor isomer in DMSO-d_6. There is no evidence of such NOEs in water and HFA solution. An earlier study also made no mention of *cis* peptide bonds for HIV Tat (1–9) in water [27].

Having assigned all the ^{1}H resonances, the ^{13}C resonances were identified from the HSQC spectra. The ^{1}H and ^{13}C chemical shifts for the peptide in both major and minor conformations are listed in Tables 2–5 respectively. There is good agreement of our data in water with the earlier NMR study of Tat (1–9) in the same medium [27].

Changes in the chemical shift of NH resonances with temperature are related to their ability to enter into H-bonds with the medium or with acceptor sites such as CO groups in the peptide (intramolecular H-bonds). Temperature coefficients of NH chemical shifts ($-\Delta\delta/\Delta T$) below 3.0 ppb are strongly suggestive of intramolecular H-bonds or solvent shielding [28]. Values above 5.0 ppb indicate that such protons are freely exposed to the solvent.

Table 3 Chemical Shifts (ppm) and Temperature Coefficients (ppb) of HIV-1 Tat (1–9) in Water

Amino acid	NH	CαH	CβH	CγH	Others	Temperature Coefficient
M^1	—	4.12	2.16	2.60	—	—
D^2	8.94	5.02	2.94, 2.71	—	—	6.3
$D^{2'}$	8.61	4.96	2.87, 2.67	—	—	5.8
$D^{2''}$	8.86	4.96	2.84, 2.71	—	—	6.5
P^3	—	4.45	2.28	2.00	δ_1H 3.85, δ_2H 3.75	—
V^4	8.09	4.04	2.02	0.93	—	8.3
$V^{4'}$	8.56	4.07	—	0.91	—	8.0
D^5	8.43	4.99	2.97, 2.76	—	—	8.9
$D^{5'}$	8.34		2.94, 2.75	—	—	—
P^6	—	4.43	2.26	2.03	δH 3.80	—
N^7	8.23	4.69	2.83, 2.74	—	NH_1 6.92, NH_2 7.59	4.7
I^8	7.86	4.19	1.90	1.44, 1.17	δH 0.91	5.7
$I^{8'}$	8.26	4.17			δH 0.89	
E^9	8.31	4.38	2.00	2.47	—	7.3

Within the range (3.0–5.0 ppb) no firm conclusion may be drawn [28]. We see that, in both DMSO-d_6 and HFA, the temperature coefficients of the NH resonance of Ile^8 only is low at 1.9 ppb (while others are beyond the limit of 5.0 ppb), pointing to its involvement in an intramolecular H-bond. There are all the strong signatures of a β-turn in the NOESY spectrum showing that the segment Asp^5-Pro^6-Asn^7-Ile^8 adopts a β-turn with the NH of Ile^8 locked in an intramolecular H-bond with the CO of Asp^5. Furthermore, the β-turn is strengthened by Pro ideally occupying the second position in the turn. The $^3J_{NH\alpha}$ coupling constants of the $(i+1)$ and $(i+2)$ residues in the β-turn are also strong indicators of a β-turn motif. For the $(i+1)$ residue this value is smaller at ~4.0 Hz, while a ~9.0 Hz coupling constant characterizes the $(i+2)$ residue in the β-turn [22]. Unfortunately, in our situation, no coupling constant could be obtained for Pro^6, nevertheless, the coupling constant for Asn^7 was close to that expected for a residue involved in a such turn. It should also be noted that both the NH and

Table 4 Chemical Shifts (ppm) and Temperature Coefficients (ppb) of HIV-1 Tat (1–9) in HFA

Amino acid	NH	CαH	CβH	CγH	Others	Temperature Coefficient
M^1	—	4.13	2.18	2.63	—	—
D^2	8.67	5.06	2.82, 2.56	—	—	6.1
P^3	—	4.45	2.29	2.01	δH 3.82	—
V^4	7.85	4.11	2.07	0.93	—	6.4
$V^{4'}$	7.99	4.13	2.07	0.97		7.0
D^5	8.06	4.91	2.87, 2.61	—	—	7.1
$D^{5'}$	7.99	4.83	2.85, 2.62			7.0
P^6	—	4.48	2.29	2.01	δ_1H 3.87, δ_2H 3.78	—
N^7	8.46	4.73	2.82	—	NH_1 6.80, NH_2 7.76	3.8
I^8	7.66	4.22	1.95	1.47, 1.22	δH 0.94	1.9
E^9	8.00	4.04	2.08, 1.95	2.29	—	6.8

Table 5 ^{13}C Chemical Shifts (ppm) of HIV-1 Tat (1–9) in DMSO-d_6 and HFA

Solvent	Amino acid	CαH	CβH	CγH	Others
DMSO	M^1	54.32	36.67	29.70	—
HFA		58.43	32.21	27.50	—
DMSO	D^2	55.71	42.93	—	—
HFA		52.69	40.67	—	—
DMSO	P^3	63.41	31.19	28.76	δ50.78
HFA		62.99	32.84	28.56	δ9.82
DMSO	V^4	61.31	34.28	24.73	—
HFA		64.75	35.11	24.16	—
DMSO	D^5	54.90	42.96	—	—
HFA		52.56	39.46	—	—
DMSO	P^6	62.54	34.16	26.88	δ1.81
HFA		62.83	34.21	25.54	δ1.52
DMSO	N^7	53.22	40.35	—	—
HFA		52.56	38.49	—	—
DMSO	I^8	59.73	40.20	27.60, 27.50	δ4.46
HFA		57.97	38.44	26.50, 26.40	δ3.24
DMSO	E^9	57.90	32.38	35.78	—
HFA		56.81	32.96	34.91	—

αH chemical shift dispersion for the sequence Asp^5-Pro^6-Asn^7-Ile^8 was nearly identical in DMSO-d_6 and HFA but differed significantly from that in water, suggesting that the conformation was similar in these two media. Thus, the peptide has an identical structure (a β-turn) at the *C*-terminal end in both DMSO-d_6 and HFA. The temperature coefficients and coupling constants in DMSO-d_6 and HFA for residues at the *N*-terminal end of the peptide, speak of a random coil structure. In water, the NMR data indicate that the peptide cannot be described by any of the classical secondary structural motifs.

Other than the aforementioned *cis* peptide bond between Asp^2 and Pro^3 for the minor isomer in DMSO-d_6, there is a very little information in the spectra to fully deduce the complete structure of the minor isomers in all three solvents.

MD Simulations

The structure simulated utilizing NMR data individually from DMSO-d_6, water (pH 2.7) and HFA showed no or very little violations in the imposed distances and dihedral restraints. The simulated structures were refined to *R* factors which are noted in Table 1. The backbone torsion angles (ϕ, φ) averaged over the *ensemble* of 25 structures for each of the three simulations are given in Table 6. It can be seen that the ϕ, φ angles for Pro^6 and Asn^7 in simulations (S1 and S3) are typical of a type I β-turn. In simulation S2, run with NMR data obtained from water, the ϕ, φ angles for the stretch of residues spanning Pro^3 to Pro^6 are close to a left-handed polyproline II (PPII) helix [29]. In general the length of a PPII helix spans 4–8 residues, with ϕ, φ values of $\sim -75^\circ$ and $\sim 145^\circ$. The PPII helix does not have the regular pattern of intramolecular H-bonds as seen in normal α-helices (and its variant), and is mainly stabilized by H-bonding with water. The PPII helix has a strong preference for Pro, but besides Pro, several other residues like Glu, Ser, Arg and Ala are well accommodated. It is now realized that many structures, which were assigned a random coil are actually a polyproline II helix. The helix is mainly identified by the torsion angles. A representation of the structures simulated using NMR data in the three solvents is given in Figs 3–5.

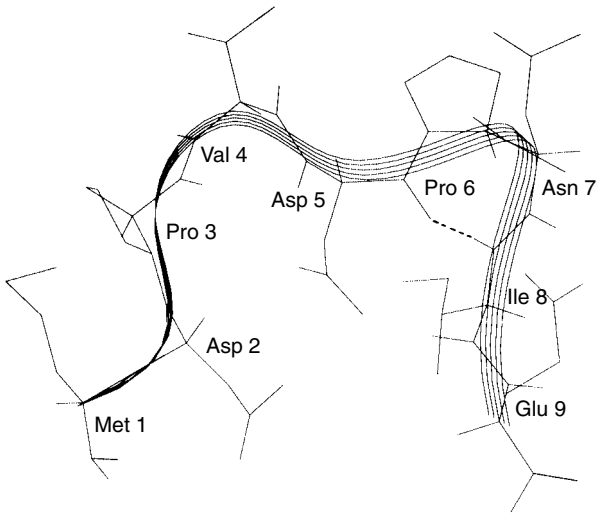

Figure 3 Structure of HIV-1 Tat in DMSO-d_6. The dotted line shows H-bonding in the β-turn. The ribbon traces the backbone atoms.

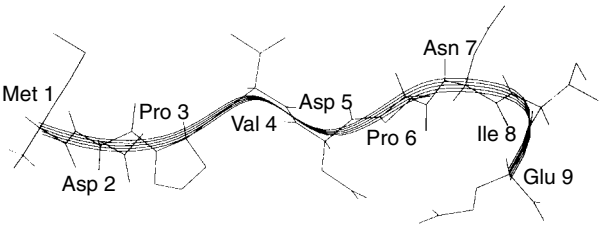

Figure 4 Structure of HIV-1 Tat in water.

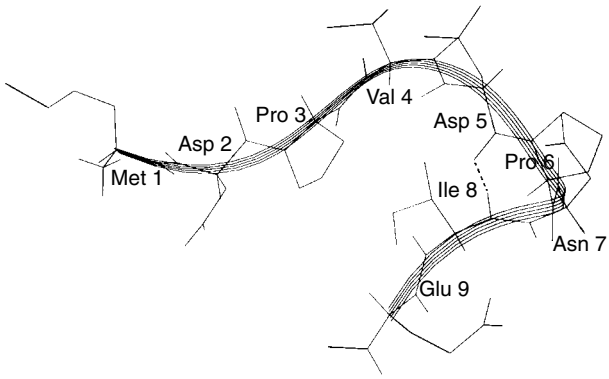

Figure 5 Structure of HIV-1 Tat in HFA. The dotted line shows H-bonding in the β-turn.

CONCLUSION

2D-NMR in conjunction with MD simulation have shown that Tat (1–9) has an identical conformation in both DMSO-d_6 and HFA solutions. This conformation is characterized by a type I β-turn around the *C*-terminal residues Asp^5-Pro^6-Asn^7-Ile^8. The *N*-terminal portion of the peptide is best described

Table 6 Backbone Torsion Angles[a] (ϕ, φ) for HIV-1 Tat (1–9) Averaged Over Entire Trajectory Obtained by Simulated Annealing

Amino acid	DMSO (S1)		Water (S2)		HFA (S3)	
	ϕ	φ	ϕ	φ	ϕ	φ
Met[1]	—	132(9)	—	176(6)	—	170(7)
		103(8)				−171(3)
Asp[2]	−99(13)	159(6)	−98(3)	125(5)	−76(5)	164(11)
	−147(5)	102(8)				
		−150(1)				
Pro[3]	−96(4)	−73(15)	−75(2)	156(2)	−113(8)	−16(8)
						166(4)
Val[4]	−126(7)	79(7)	−92(1)	168(0)	−76(5)	−94(27)
					−117(10)	
Asp[5]	−145(11)	64(12)	−90(0)	132(0)	−114(12)	108(17)
	−117(8)					
Pro[6]	−60(0)	−29(0)	−74(0)	161(0)	−60(1)	−26(0)
Asn[7]	−88(0)	0(0)	−110(0)	25(0)	−85(0)	2(1)
Ile[8]	−149(2)	120(1)	−108(0)	115(0)	−136(3)	120(5)
Glu[9]	−164(1)	—	−95(0)	—	−152(1)	—

[a] Torsion angles are in degrees. In parenthesis is the RMSD.

as a random coil. In water, the peptide adopts a left-handed polyproline II (PPII) helix around the mid segment region covering residues Asp[2] to Pro[6].

As stated earlier, there is a report of a ^{1}H NMR conformational study of Tat (1–9) and its variants in water [27]. The proton chemical shift and NH temperature coefficients reported by them are close to the values noted in this work. However, simulated structures reported by them have ϕ, φ values that are slightly different from ours. They have inferred a 'flexible structure' for Tat (1–9) in water. A close inspection of the ϕ, φ values for residues Asp[2], Pro[3], Asp[5] and Ile[8] reported by them are in fact the standard values of a PPII helix [29] and should better be described as a polyproline helix and not a 'flexible conformation'.

Based on their NMR data, they have also suggested the propensity of Ile[5] and Ile[8] to form a turn or turn-like structure, but have not elaborated on this feature. Our NMR data for the peptide in DMSO-d_6 and HFA reveal very firmly that this 'turn like structure' is in fact a well characterized β-turn.

Acknowledgement

The facilities provided by the National Facility for High Field NMR located at TIFR and supported by the Department of Science and Technology (DST) are gratefully acknowledged. We also thank the All India Council of Technical Education (AICTE), New Delhi for the computational facilities at BCP. MK thanks CSIR for a senior research fellowship.

REFERENCES

1. Sodroski JG, Rosen CA, Goh WC, Haseltine WA. A transcriptional activator protein encoded by the X-lor region of the human T-cell leukemia virus. *Science* 1985; **28**: 1430–1434.
2. Dayton AI, Sodroski JG, Rosen CA, Goh WC, Haseltine WA. The trans-activator gene of the human T cell lymphotropic virus type III is required for replication. *Cell* 1986; **44**: 941–947.
3. Ensoli B, Buonaguro L, Barillari G, *et al.* Release, uptake and effects of extracellular human immunodeficiency virus type 1 Tat protein on cell growth and viral transactivation. *J. Virol.* 1993; **67**: 277–287.
4. Viscidi RP, Mayur K, Lederman HM, Frankel AD. Inhibition of antigen-induced lymphocyte proliferation by Tat-protein from HIV-1. *Science* 1989; **246**: 1606–1608.
5. Subramanyam M, Gutheli WG, Bachovchin WW, Huber BT. Mechanism of HIV-1 Tat induced inhibition of antigen-specific T-cell responsiveness. *J. Immunol.* 1993; **150**: 2544–2553.
6. Heins J, Neubert K, Barth A, Canizaro PC, Behal FJ. Kinetic investigation of the hydrolysis of aminoacyl *p*-nitro-anilides by dipeptidyl peptidase IV from human

and pig kidney. *J. Biochim. Biophys. Acta* 1984; **785**: 30–36.
7. Gutheil WG, Subramanyam M, Flentke GR, *et al.* Human immunodeficiency virus -1 Tat binds to dipeptidyl aminopeptidase IV (CD26): A possible mechanism for Tat's immunosuppressive activity. *Proc. Natl. Acad. Sci. USA* 1994; **91**: 6594–6598.
8. Wrenger S, Hoffmann T, Faust J, *et al.* The N-terminal structure of HIV-1 Tat is required for suppression of CD26-dependent T cell growth. *J. Biol. Chem.* 1997; **272**: 30283–30288.
9. Wrenger S, Reinhold D, Hoffmann T, *et al.* The N-terminal X-X-Pro sequence of the HIV-1 Tat protein is important for the inhibition of dipeptidyl peptidase IV (DP IV/CD26) and the suppression of mitogen-induced proliferation of human T cells. *FEBS Lett.* 1996; **383**: 145–149.
10. Buck M. Trifluroethanol and colleagues: Cosolvents come of age: Recent studies with peptides and proteins. *Quart. Rev. Biophys.* 1998; **31**: 297–355.
11. Rajan R, Awasthi SK, Bhattacharya S, Balaram P. Teflon-coated peptides — hexafluoroacetone trihydrate as a structure stabilizer for peptides. *Biopolymers* 1997; **42**: 125–128.
12. Piantini U, Sorenson OW, Ernst RR. Multiple quantum filters for elucidating NMR coupling networks. *J. Am. Chem. Soc.* 1982; **104**: 6800–6801.
13. Braunschweiler L, Ernst RR. Coherence transfer by isotropic mixing: Application to proton correlation spectroscopy. *J. Magn. Reson.* 1983; **53**: 521–528.
14. Macura S, Huang Y, Suter D, Ernst RR. Two-dimensional chemical exchange and cross-relaxation spectroscopy of coupled nuclear spins. *J. Magn. Reson.* 1981; **43**: 259–281.
15. Dhallium C, Wieruszeski JM, Lippens G. An improved homonuclear TOCSY experiment with minimal water saturation. *J. Magn. Reson. Series B* 1996; **111**: 168–170.
16. Lippens G, Dhallium C, Wieruszeski JM. Use of a water flip-back pulse in the homonuclear NOESY experiment. *J. Biomol. NMR* 1995; **5**: 327–333.
17. States DJ, Habercorn RA, Ruben DJ. A two-dimensional nuclear overhauser experiment with pure absorption phase in four quadrants. *J. Magn. Reson.* 1982; **48**: 286–292.
18. Kay IE, Keifer P, Saarinen T. Pure absorption gradient enhanced heteronuclear single quantum correlation spectroscopy with improved sensitivity. *J. Am. Chem. Soc.* 1992; **114**: 10663–10665.
19. Maple J, Dinur U, Hagler AT. Derivation of force field for molecular mechanics and dynamics from ab-initio energy surfaces. *Proc. Natl. Acad. Sci. USA* 1988; **85**: 5350–5354.
20. Verlet L. Computer experiments on classical fluids. I. Thermodynamical properties of Lennard-Jones molecules. *Phys. Rev.* 1967; **159**: 98–103.
21. Berendsen HJC, Postma JPM, van Gunsteren WF, DiNola A, Haak JR. Molecular dynamics with coupling to an external bath. *J. Chem. Phys.* 1984; **81**: 3684–3690.
22. Wüthrich K. *NMR of Proteins and Nucleic Acids*. John Wiley and Sons: New York, 1986.
23. Pardi A, Billeter M, Wuthrich K. Calibration of the angular dependence of the amide proton-C_α proton coupling constants, $^3J_{HN\alpha}$, in a globular protein. *J. Mol. Biol.* 1984; **180**: 741–751.
24. Boelens R, Koning TMG, Kaptein R. Determination of biomolecular structure from proton-proton NOE's using a relaxation matrix approach. *J. Mol. Str.* 1988; **82**: 299–311.
25. Borgias BA, James TL. Mardigras — a procedure for matrix analysis of relaxation for discerning geometry of an aqueous structure. *J. Magn. Reson.* 1990; **87**: 475–487.
26. Govil G, Hosur RV. *Conformation of Biological Molecules: New Results from NMR*. Springer-Verlag: Mannheim, 1982.
27. Mrestani-Klaus C, Fengler A, Brandt W, *et al.* ^{1}H NMR conformational study on N-terminal nonapeptide sequences of HIV-1 Tat protein: A contribution to structure-activity relationships. *J. Pept. Sci.* 1998; **4**: 400–410.
28. Bach II AC, Eyermann CY, Gross JD, *et al.* Structural studies of a family of high affinity ligands for GPIIb/IIIa. *J. Am. Chem. Soc.* 1994; **116**: 3207–3219.
29. Adzhubei AA, Sternberg MJE. Left handed polyproline helices commonly occur in globular proteins. *J. Mol. Biol.* 1993; **229**: 472–493.

